Gait Collector: An Automatic Gait Data Collection System in Conjunction with an Experience-based Long-run Exhibition

Yasushi Makihara, Takuhiro Kimura, Fumio Okura, Ikuhisa Mitsugami, Masataka Niwa,
Chihiro Aoki, Atsuyuki Suzuki, Daigo Muramatsu, Yasushi Yagi
The Institute of Scientific and Industrial Research, Osaka University
8-1 Mihogaoka, Ibaraki, Osaka, 567-0047, JAPAN
{makihara,kimura,okura,mitsugami,niwa,c-aoki,a-suzuki,muramatsu,yagi}@am.sanken.osaka-u.ac.jp

Abstract

Biometric data collection is an important first step toward biometrics research practice, although it is a considerably laborious task, particularly for behavioral biometrics such as gait. We therefore propose an automatic gait data collection system in conjunction with an experience-based exhibition. In the exhibition, participants enjoy an attractive online demonstration of state-of-the-art video-based gait analysis comprising intuitive gait feature measurement and gait-based age estimation while we simultaneously collect their gait data along with informed consent. At the time of this publication, we are holding the exhibition in association with a science museum and have successfully collected the gait data of 47,615 subjects over 246 days, which has already exceeded the size of the largest existing gait database in the world.

1. Introduction

Gait recognition [26] is a behavioral biometric that is available even at a distance from the camera, when other biometrics may be occluded, obscured, or suffer from insufficient image resolution (e.g., a face that is blurred or occluded by a mask). Because gait recognition does not require subject cooperation thanks to its non-invasive capture process, it is expected to be applied to criminal investigation from CCTV footage in public and private spaces. In fact, there is already research on using gait biometrics as a forensic tool [3, 7, 14].

Gait recognition studies involve a variety of stages: data collection, preprocessing, feature extraction, matching, and system development. Among these, the data collection stage is increasingly important because of the recent rapid progress of machine learning techniques. Robust approaches to gait recognition must be robust against covariates such as view, speed, clothing, and carrying status, and indeed, the most robust approaches to gait recognition, adopt machine learning techniques, e.g., matrix factorization [19, 25], manifold learning [1, 22], subspace learning [11, 13], discriminant analysis [2, 23], support vector machines (SVMs) [10, 24], and neural networks [9]. In addition, a large-scale gait database is essential for the statistically reliable performance evaluation of gait recognition [8] as well as the construction of a reliable probability density function of genuine subjects and imposters for forensic purposes [7].

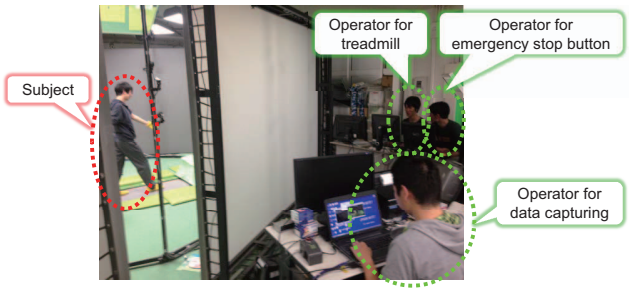

Figure 1: Data collection experiment setup for the OU-ISIR Treadmill dataset [15], where three operators are needed to run the system.

Gait data collection at a large scale is an extremely laborious and costly task, because gait data are essentially composed of videos, and hence both data collectors and subjects need to be engaged in data collection experiments for long periods of time, compared with other biometrics obtained from still images (e.g., fingerprints, irises, and faces).

To gain a deeper understanding of this issue, imagine the data collection process for a certain gait database, for example, the OU-ISIR Treadmill dataset [15]. First, subjects must be found (e.g., volunteers or part-time workers) through advertisement. Second, the aim of data collection experiments must be explained and informed consent ob-

978-1-5090-1869-7/16/$31.00 ©2016 IEEE

tained (e.g., a signed release agreement) from the subjects. After the subjects have sufficiently practiced walking on the treadmill, their gait data may be collected with the cooperation of multiple operators for the treadmill, video capture software, and emergency stop button (see Fig. 1). It is therefore difficult to collect a large number of subjects with this kind of setup.

To overcome this difficulty, collecting gait data in conjunction with an experience-based exhibition of video-based gait analysis is an option, where a large number of participants visit, even without any explicit calls for subjects (The terms participant and subject are used interchangeably from the viewpoints of the experience-based exhibition and gait data collection in this paper.). In fact, the world's largest gait database, the OU-ISIR Large Population dataset [8], which contains more than 4,000 subjects, was constructed through such exhibitions, i.e., several-day exhibitions in a science museum or on an open campus. However, this framework does not solve the other aspect: substantial personnel are still required to operate the gait capturing software, check the baggage of the participants, and annotate the result of video-based gait analysis. It is therefore difficult to continue this data collection for long periods of time.

Another choice is to collect gait data by installing a camera to observe a well-trafficked street or somewhere similar and by continuously recording the scene without any personnel on site. This approach, however, still suffers from laborious post-processing: the manual segmentation of individual subjects and annotation of the subject IDs for each individual. Moreover, because the captured subjects are general people without any informed consent, the data capture itself may be problematic from the viewpoint of ethical, legal, and social issues (ELSI) (e.g., the protection of privacy and personal information).

To construct an extremely large-scale gait database while taking the above points into account, we propose an automatic gait data collection system in conjunction with an experience-based long-run exhibition of video-based gait analysis[1]. Note that this paper focuses not on the database itself but on the system to collect gait data in large scale. The contributions of this work are three-fold.

1. An online demonstration of state-of-the-art video-based gait analysis

A key to the success of collecting a large number of participants depends on an attractive demonstration. We therefore developed an online demonstration system of state-of-the-art video-based gait analysis composed of two main components: (1) measurement of intuitive gait features such as walking speed, stride, arm swing, and motion symmetry, and (2) gait-based age estimation. The participants are given the opportunity to receive a printed card of their personal gait measurement results as well as to compare their results in a group such as with family and friends, which can be an incentive for participation.

2. An automatic gait data collection system

In order that the participants can enjoy the demonstration by themselves and that the gait data can be collected without any manual operation, we developed an automatic system where a QR code is used to maintain subject ID and trigger the demonstration, photo-electronic sensors are used for passage detection to trigger various events, and speakers for audio guidance are used so that the participant can easily understand the next action they should take.

3. Data collection with informed consent

The system also provides a function to obtain informed consent from the participants so that the collected data can be used for research purposes, which was carefully implemented under supervision by a lawyer familiar with ELSI. Therefore, the collected gait database can be made available in the public domain to advance state-of-the-art video-based gait analysis in the future.

2. Automatic gait data collection system

2.1. Overview

A system overview is given from a participant's viewpoint along with Fig. 2. The participant first reads an explanation of the aim of the experience-based exhibition in parallel with gait data collection at the entrance panel. The participant then goes into the demonstration site and visits a QR-code ticket machine (Fig. 3(a)), where more detailed explanation about the exhibition is provided. A QR code that includes an assigned subject ID is issued to participants after they input gender and age information. They subsequently enter the line for the online demonstration of video-based gait analysis. They pass the QR code over the QR-code reader (Fig. 3(b)) and then enter a walking course in accordance with audio guidance, where a green chroma-key background is installed.

The participant then walks to the other side, carrying any items such as bags or backpacks, and then places these items into a box. Subsequently, he or she walks two more rounds and then picks up the items and leaves the walking course. At the exit of the walking course, participants check the result of video-based gait analysis through a display and obtain a printed result if they press a button to agree to the research purpose use of their gait data (Fig. 3(c)). Furthermore, they can also compare the results with their family members or friends through another display (Fig. 3(d)).

2.2. Demonstration unit

The demonstration unit comprises two processes: intuitive gait feature measurement and gait-based age estima-

[1] "Just from walking", the 15th media lab. at Miraikan (one of the largest science musiumi in Japan), from 15th Jul. 2015 to 27th Jun. 2016,

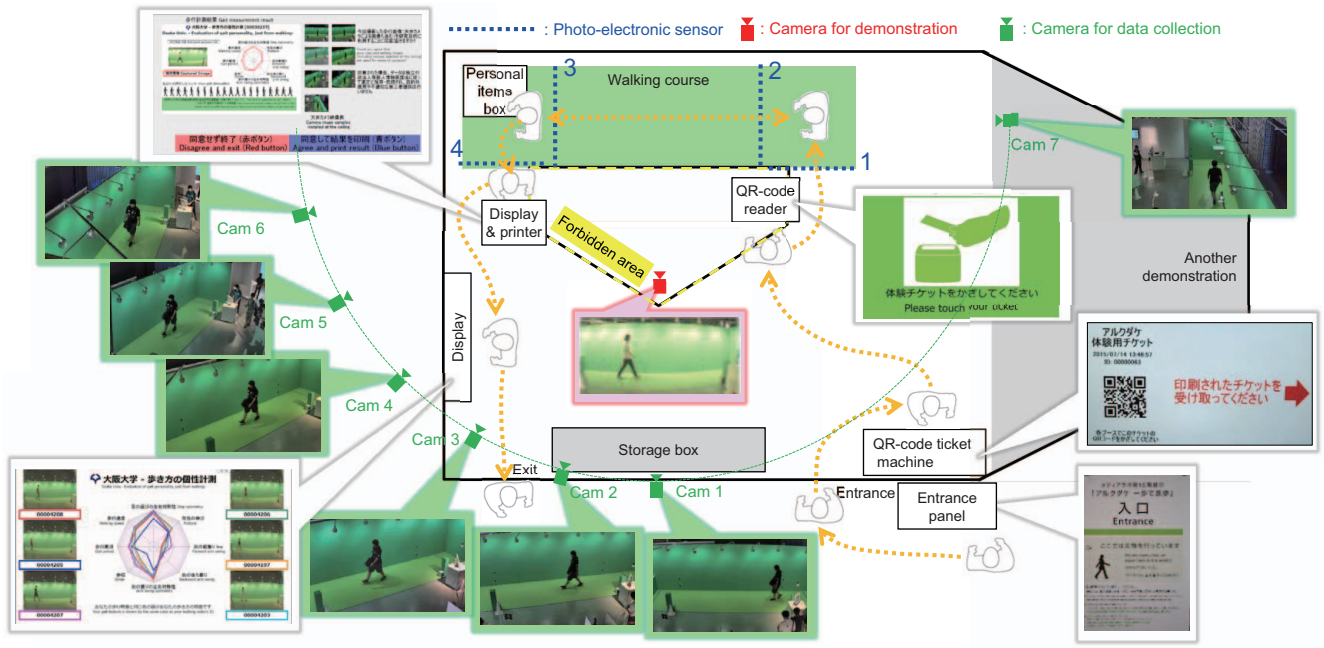

Figure 2: System overview. A bilingual explanation is presented at each site.

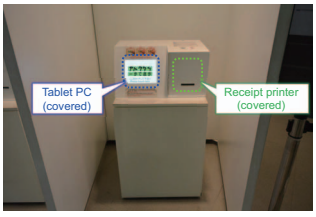

(a) QR-code ticketing machine

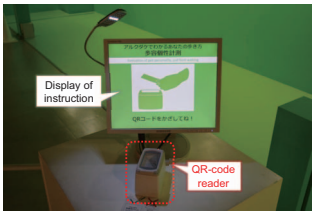

(b) QR-code reader

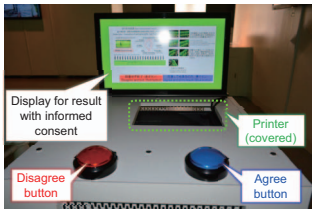

(c) Display and printer

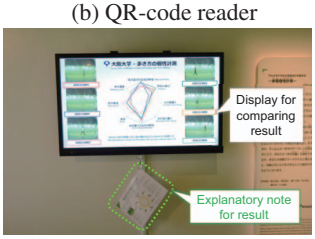

(d) Display for comparing result

Figure 3: Key components of the exhibition.

tion. We implement the two processes using left-to-right 2.5-s walking image sequences (The start time for capture is determined by photo-electronic sensors, as described later.) of 640 × 480 pixels at 30 fps, captured by a USB camera (PointGrey, FMVU-13S2C-CS). Because both processes rely on silhouette-based analysis, silhouette extraction is an important preprocessing step. For this purpose, the demonstration unit implements (1) region of interest (ROI) setting, (2) background subtraction with pixel-wise single Gaussian background modeling, and (3) color-based pixel-wise shadow removal, as shown in Figs. 4(a) and (b) (A simplified version of [20] was implemented.). The ROI and thresholds for the preprocessing can be adjusted through a graphical user interface (e.g., a scroll bar) while confirming the results online, which enables us to easily adapt the system to a particular demonstration site.

Intuitive gait feature measurement

In the following paragraphs, intuitive gait feature measurement is briefly described (see [17] for more technical detail). We consider eight intuitive gait features: walking speed, gait period, stride, step symmetry, forward arm swing, backward arm swing, arm swing symmetry, and posture. We first apply morphological operation and max-region filtering to obtain the silhouette sequence as well as the bounding box sequence of the participant. Because the camera used for this demonstration is calibrated in advance and the ground plane constraint on the foot point is available, the walking speed is easily computed from the traveling distance between the start and end foot positions in the world coordinates and elapsed time (i.e., 2.5 s).

We then compose a size-normalized silhouette sequence (Fig. 4(c)) and compute a gait period by maximizing the normalized auto-correlation along with the temporal axis [18]. Furthermore, we detect a series of single support phases (SSPs) and double support phases (DSPs), where arms and legs are the most closed and spread, respectively (Fig. 4(d)(e)). Subsequently, we compute individual strides between adjacent DSPs based on the traveling distance and elapsed time. We then compute their average to determine the stride and also compute the deviation as the left-right

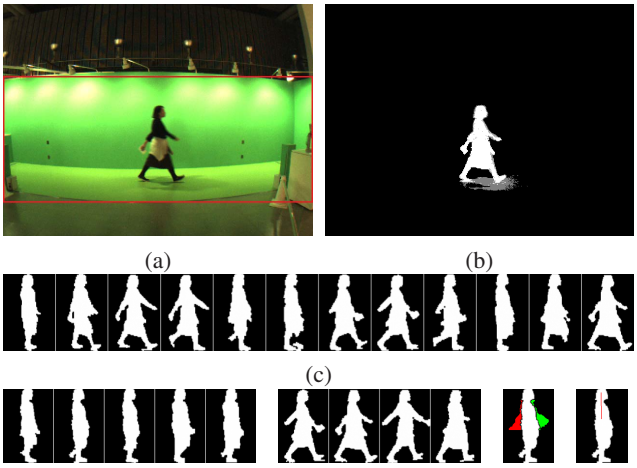

Figure 4: Intuitive gait feature measurement. From an original image and ROI (red rectangle) in (a), a silhouette (white) and shadow (gray) are extracted in (b). A size-normalized silhouette sequence (every three frames) is shown in (c), and detected SSPs and DSPs for all the steps are shown in (d) and (e), respectively. Areas swept by the arm swing are superimposed on an SSP frame (green: forward and red: backward) in (f) and a central line segment from the head to upper torso for posture measurement is depicted by a red line in (g).

step asymmetry.

We next extract front-side and back-side lines of the torso from an SSP frame and compute the areas swept by the arms in front of the front-side line and behind the back-side line as forward and backward arm swings, respectively (Fig. 4(f)). Thereafter, the deviation of the areas swept by arms between pairs of adjacent SSPs is regarded as the let-right arm swing asymmetry. Finally, we compute the central line segment from the head to the upper torso; this inclination is used to measure the goodness of posture (Fig. 4(g)).

Gait-based age estimation

In the following paragraphs, gait-based age estimation is briefly described and we refer the readers to [16] for more details about the baseline component.

We first extract the gait energy image (GEI) [5], i.e., the averaged silhouette [12], as a gait feature by averaging the size-normalized silhouette sequence for one gait period. Here, we unfold the GEI into a feature vector $\boldsymbol{x} \in \mathbb{R}^M$, where M is the dimension of the feature vector, i.e., the image size of the GEI. We then adopt Gaussian process regression (GPR) [4] as an example-based approach to age estimation.

For this purpose, let us assume that a training set $D = [X, \boldsymbol{y}]$ is given, where $X = [\boldsymbol{x}_1, \cdots, \boldsymbol{x}_N]$ is a set of N samples of gait features and $\boldsymbol{y} = [y_1, \cdots, y_N]$ is a set of the corresponding ground truth ages. In addition, an affinity function, i.e., an inner product between two feature vectors $\boldsymbol{x}_i$ and $\boldsymbol{x}_j$ is defined as a radial basis function (RBF) kernel so as to cope with the nonlinearity,

$$k(\boldsymbol{x}_i, \boldsymbol{x}_j; r) = \exp\left(-\frac{||\boldsymbol{x}_i - \boldsymbol{x}_j||}{2r^2}\right), \quad (1)$$

where $\|\cdot\|$ is the L_2 norm and r is a hyper-parameter for the RBF kernel.

Thereafter, given an input gait feature $\boldsymbol{x}_*$, the GPR estimates the posterior probability distribution of age y_* corresponding to gait feature $\boldsymbol{x}_*$ based on training set D. According to the theory of Gaussian processes, the posterior probability distribution $P(y_*|\boldsymbol{x}_*, D)$ is defined as a Gaussian distribution $\mathcal{N}(y_*; \mu_y, \sigma_y^2)$, where mean μ_y and variance σ_y^2 are defined as

$$\mu_y = \boldsymbol{k}_*^T (K+S)^{-1} \boldsymbol{y} \quad (2)$$

$$\sigma_y^2 = k(\boldsymbol{x}_*, \boldsymbol{x}_*) - \boldsymbol{k}_*^T (K+S)^{-1} \boldsymbol{k}_* + \sigma^2, \quad (3)$$

where K is an $N \times N$ square matrix whose (i,j)-th component is $k(\boldsymbol{x}_i, \boldsymbol{x}_j)$, $\boldsymbol{k}_*$ is an N-dimensional vector whose i-th row is $k(\boldsymbol{x}_i, \boldsymbol{x}_*)$, S is an $N \times N$ diagonal matrix whose (i,i)-th component is σ^2, and σ^2 is observation noise variance for age, which is experimentally set as $\sigma^2 = 0.25$.

In Eqs. (2) and (3), the most time consuming part is computing the inverse of an $N \times N$ matrix, i.e., $(K+S)^{-1}$, which has a computational time complexity of $\mathcal{O}(N^3)$ and may make online computation difficult. We therefore employ a GPR with dynamic active set method [29], where the training set used is limited to the neighborhood of the input vector $\boldsymbol{x}_*$. For example, if we choose $K (\ll N)$ nearest neighbors to the input vector $\boldsymbol{x}_*$, the computational time complexity is $\mathcal{O}(K^3)$ for the inverse matrix computation, which is much less complex than $\mathcal{O}(N^3)$, i.e., computationally tractable for an online demonstration.

On the other hand, a too-small K may degrade the accuracy of the gait-based age estimation, and hence we need to choose a suitable K while considering the tradeoff between accuracy and computational efficiency. We therefore conducted preliminary experiments to investigate the tradeoff using a subset of the OU-ISIR Large Population dataset, Camera 1, Version 2 (OULP-C1V2) [8], which contains $N = 1,678$ training subjects and 2,257 test subjects. Consequently, we determined the number of nearest neighbors to be $K = 10$. In addition, parameter r for the RBF kernel is defined by taking the proximity of the chosen nearest neighbors into account as

$$r = \frac{1}{K} \sum_{k=1}^{K} \|\boldsymbol{x}_{kNNID(k)} - \boldsymbol{x}_*\|, \quad (4)$$

where $kNNID(k)$ is a training sample index of the k-th nearest neighbor to the input $\boldsymbol{x}_*$.

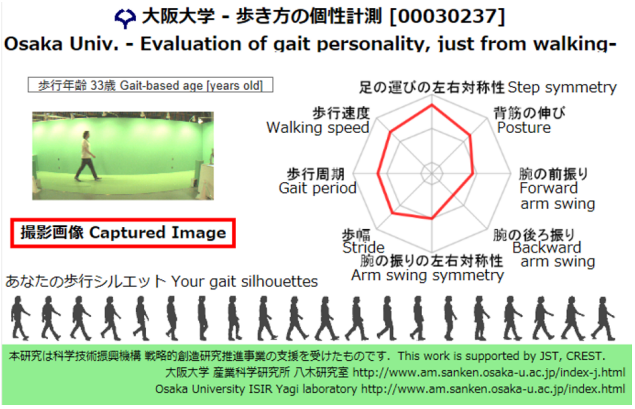

(a) Printed card for each participant.

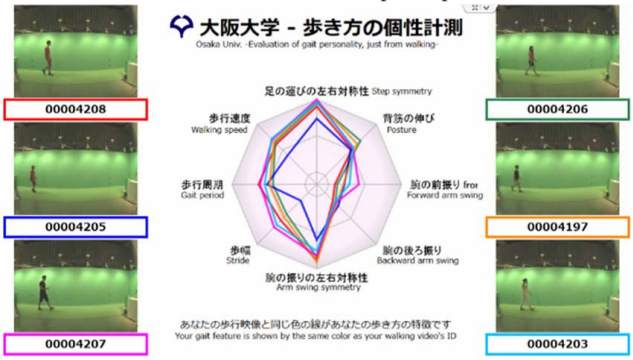

(b) Comparison among six latest participants.

Figure 5: Display presented to the participants. In (a), the measured intuitive gait features are shown by a radar chart and inner, middle, and outer octagons indicate the minimum, average, and maximum values for each intuitive gait feature, respectively. In (b), the measured intuitive gait features are shown in a common radar chart using colors corresponding to individual participants.

Display to the participants

The results obtained by the intuitive gait feature measurement and gait-based age estimation are displayed to the participants in two ways. One is a printed card that contains measured intuitive gait features and estimated gait-based age as well as a captured original image and a size-normalized silhouette sequence for each participant (Fig. 5(a)). The other is a comparison of measured intuitive gait features and captured original videos of the six most recent participants, where each participant is highlighted by a corresponding color (Fig. 5(b)).

2.3. Data collection unit

While the participant experiences the demonstration at the walking course, gait data of 1,280 × 960 pixels at 25 fps are captured by seven network cameras (AXIS Communications, Q1614) placed at intervals of 15-deg azimuth angles along a quarter of a circle whose center coincides with

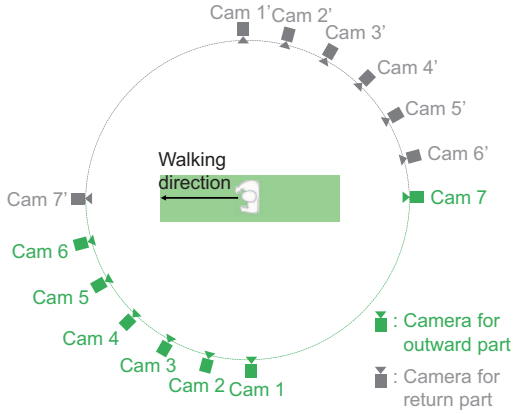

Figure 6: Illustration of the camera setup.

the center of the walking course. Its radius is approximately 8 m and height is approximately 5 m (Fig. 2). One exception is the camera for the front/back-view (Cam 7), which is placed on the opposite side of the other cameras to avoid occlusion by a brace for the green chroma-key structure.

As introduced in Section 2.1, each participant first walks to the personal items box and puts his or her bags it into it, and then walks two more rounds. Note that the observed view from the cameras to the participant for the return part is regarded simply as the opposite of that for the outward part. More specifically, the participant is observed from the side-to-frontal view on the left side and also from the back for the outward part (Cam 1 to Cam 7 in Figs. 2 and 6), and then from the side-to-back view on the right side and also from the front for the return part (Cam 1' to Cam 7' in Fig. 6).

As a result, a walking sequence with carrying status is observed for the outward part (seven views) as well as two normal walking sequences for each of the outward and return parts (14 views in total). We can therefore evaluate the gait recognition algorithms under a number of protocols, for example, gait recognition under the same covariate condition, multi-view and cross-view gait recognition, and gait recognition with and without carrying status. In addition, we can also use the data for other video-based gait analyses, e.g., gait-based gender classification and age estimation.

Because each network camera continuously records the walking course during the opening hours of the demonstration booth, we need to segment the video into pieces containing individual subjects with corresponding subject IDs. For this purpose, we exploit the log from the QR-code reader at the entrance to obtain the subject ID, and also photo-electronic sensors to obtain the time the subject passes them. More specifically, because we installed four photo-electronic sensors at: (1) the entrance, (2) the start line of the outward part, (3) the start line of the return part,

and (4) the exit, as shown in Fig. 2, we can pick up individual walking sequences for the outward and return parts, which total five sub-sequences for each subject.

2.4. Informed consent

Because we want to use the collected gait data for our research as well as to make it available in the public domain to facilitate video-based gait analysis in the research community, it is quite important to obtain informed consent for the research-purpose use of the collected gait data from the participants. For this purpose, we consulted with a lawyer who is an authority on ELSI with respect to CCTVs as to how to appropriately obtain the informed consent, and further obtained advice on a number of items ranging from a comprehensive viewpoint (i.e., the ground design of the experience-based exhibition) to a specific viewpoint (i.e., the specific text to be presented to the participants).

More specifically, announcements regarding the informed consent are repeatedly presented to the participant at three sites. The first site is the entrance panel, which informs the participants of the aim of the experience-based exhibition of video-based gait analysis in parallel to the gait data collection. The second site is the QR-code ticketing machine, where a similar explanation is presented to the participant on a tablet PC, and a QR code is issued only if the participant agrees to it. Moreover, if the participant is a child, we request that a guardian read the explanation and decide whether to agree on behalf of the child.

The third site is the display and printer at the exit of the walking course. Here, we show a number of items: (1) the result to be printed, (2) sample images captured by the seven network cameras, and (3) an explanation of its research purpose use and appropriate management based on privacy laws. At this site, we installed physical buttons by which participants declare agreement (a blue button) or disagreement (a red button) to this use of their data (Fig. 3(c)). If the participant presses the agree button, the result is printed (Fig. 5(a)) and also appears in the display for comparison (Fig. 5(b)), otherwise, the result is not printed and does not appear on the display.

3. Results and discussion

3.1. Computational time

The online process is an important aspect of the demonstration, and hence we evaluated the computational times for the two components: intuitive gait feature measurement and gait-based age estimation. As a result, computational times averaged over ten trials are 1.5 and 0.2 s, respectively. These two components begin processing just after the participant completes the first return part. Thereafter, the participant walks one and a half rounds more, which clearly takes much more time than the total processing time (1.7 s). Therefore, when the participant leaves the walking course, the result has been already displayed, i.e., the participant needs not wait for the result. Consequently, we conclude that the computational time is acceptable for the online demonstration.

3.2. Accuracy of gait-based age estimation

Another important aspect is the accuracy of the measured/estimated results. Because there is no ground truth for the intuitive gait features, we evaluated the gait-based age estimation by comparing it with the participant's input age at the QR-code ticketing machine.

More specifically, we evaluated the accuracy by the mean absolute error (MAE) between the estimated ages and the ground truth ages, with a subset of collected data (5,298 subjects). As a result, we obtained 8.44 years MAE, which is almost the same as that using the baseline algorithm (MAE: 8.4 years) reported in [16]. Since it takes more than 30 s for gait-based age estimation if we use the full training set without the active set method in the same way as [16], which was confirmed by a preliminary experiment, it turns out that our active set-based method realizes a good tradeoff between the accuracy and computational cost for gait-based age estimation.

3.3. Rate of agreement to the research purpose use

In order to know how our gait demonstration system attracts the participants, we investigate the rate of agreement to the research purpose use of their gait data. As a result, 97.8% of the participants agreed to it and obtained the printed results of the intuitive gait feature measurement and gait-based age estimation, which shows that our demonstration of video-based gait analysis can be a good incentive for participation.

This implies a possibility that other biometric researchers can also automatically collect large-scale biometric data with informed consent in a similar framework if they provide an attractive biometric experience-based exhibition (e.g., facial age progression simulation or facial expression editing for face biometrics) in a right place such as a science museum.

3.4. Data collection progress

As of this publication, we have run the exhibition and collected the gait data of 47,615 subjects for 246 days. Because the largest existing gait database in the world contains 4,016 subjects [8], the collected gait dataset has already exceeded it in size. Because we plan to continue the long-run exhibition for approximately 11 months in total, we expect that the number of subjects will ultimately exceed 70,000 in number.

As a reference, subject statistics in terms of gender and age are shown in Fig. 7. We can see that a wide range

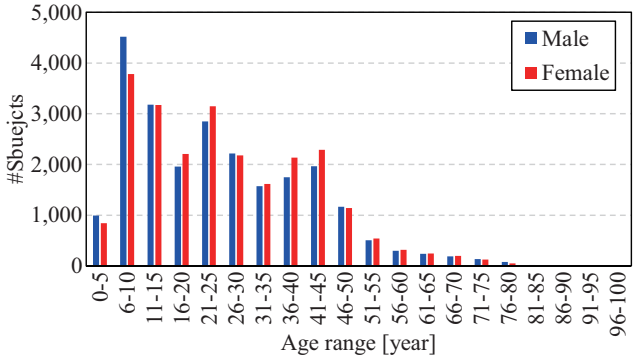

Figure 7: Subject statistics.

of ages and gender are covered except adults over 60 years old. Because we are now planning to invite a group of older adults (over 60 years old) to participate in the exhibition, the biased age distribution is expected to be more or less improved.

3.5. Prospective use of collected data

Before discussing prospective use of the collected data, we briefly review the existing gait databases. Important aspects for gait databases are (1) a large number of subjects and (2) a variety of covariate conditions. Some publicly available gait databases, such as the USF gait database [27], SOTON gait database [28], CASIA gait database [30], OU-ISIR Treadmill dataset [15], and TUM GAID [6], contain several covariate conditions, such as views, clothing, and carrying conditions. They do not, however, contain a sufficient number of subjects (i.e., at most 100 orders). The only exception is the OU-ISIR large population dataset [8], which contains over 4,000 subjects. It does, however, not contain a sufficient covariate conditions (i.e., relatively limited view variations from 55 deg to 85 deg). Moreover, we cannot say that the database with approximately 4,000 subjects is extremely large-scale.

On the other hand, we will collect over 70,000 subjects by the end of the exhibition, with covariate conditions of views and carrying status, which meets the important aspects for the gait database.

Such an extremely large number of subjects are beneficial for video-based gait analysis. For instance, we can use the collected data as training samples for example-based approaches to gait-based age or gender estimation such as GPR-based age estimation [16] used in this system.

Moreover, as for gait recognition task, it is well known that standard deviation of false rejection rate (FRR) in a verification scenario is approximately inverse proportion to the squared root of $N-1$, where N is the number of subjects in probes [21]. We can hence reduce the standard deviation of FRR approximately by one-fourth compared with the OU-ISIR large population dataset [8] (i.e., $\sqrt{4000/70000} \approx 1/4$), which means 4-times statistically reliable performance of gait recognition is possible.

In addition, because the collected data contain the variations of view and carrying status with approximately 100-times larger number of subjects than the existing gait database with covariate factors [6, 15, 27, 28, 30], we expect to improve the accuracy of machine learning-based approaches to robust gait recognition [10, 18, 23, 24] when the collected data are used as training samples.

3.6. Limitations

While it is usually preferable to collect an enrollment (gallery) and a query (probe) of biometric data from different sessions within a certain time lapse, the collected gait data contain few time lapses. This is an inevitable limitation of this kind of data collection framework because we cannot control the participants' revisits in principle. To promote revisits, we need to seek more repeater-oriented contents for the exhibition (e.g., a regular health checkup by video-based gait analysis) as well as to issue a more robust ID card for repeated use instead of a receipt with a QR code for single-day use.

Moreover, development of the automatic data collection system is more costly than manual data collection. However, this should be considered as a tradeoff between the initial cost and running cost with respect to both budget and personnel. We believe that our choice, i.e., high initial cost but low running cost, is suitable when collecting extremely large-scale gait datasets.

4. Conclusion

This paper addresses an automatic gait data collection system in conjunction with an experience-based exhibition. We collected participants' gait data with informed consent while they enjoyed the online demonstration of state-of-the-art video-based gait analyses: intuitive gait feature measurement and gait-based age estimation. Finally, as of this publication, we have actually run the experience-based exhibition with the cooperation of a science museum and collected the gait data of 47,615 subjects.

After the long-running exhibition ends, we will construct an extremely large-scale gait database and evaluate a number of standard video-based gait analysis algorithms. The dataset will then be made available to the public to advance state-of-the-art gait research.

Acknowledgment

This work was partly supported by JSPS Grants-in-Aid for Scientific Research (A) 15H01693, Scientific Research (B) 16H02848, and the JST CREST "Behavior Understanding based on Intention-Gait Model" project. We also appreciate Miraikan staff for this opportunity of data collection in conjunction with a long-run exhibition.

References

[1] N. Akae, A. Mansur, Y. Makihara, and Y. Yagi. Video from nearly still: an application to low frame-rate gait recognition. In *Proc. of the 25th IEEE Conf. on Computer Vision and Pattern Recognition (CVPR 2012)*, pages 1537–1543, Providence, RI, USA, Jun. 2012.

[2] K. Bashir, T. Xiang, and S. Gong. Gait recognition without subject cooperation. *Pattern Recognition Letters*, 31(13):2052–2060, Oct. 2010.

[3] I. Bouchrika, M. Goffredo, J. Carter, and M. Nixon. On using gait in forensic biometrics. *Journal of Forensic Sciences*, 56(4):882–889, 2011.

[4] C. K. I. W. Carl Edward Rasmussen. *Gaussian Processes for Machine Learning*. The MIT Press, 2006.

[5] J. Han and B. Bhanu. Individual recognition using gait energy image. *IEEE Trans. on Pattern Analysis and Machine Intelligence*, 28(2):316– 322, 2006.

[6] M. Hofmann, J. Geiger, S. Bachmann, B. Schuller, and G. Rigoll. The tum gait from audio, image and depth (gaid) database: Multimodal recognition of subjects and traits. *J. Vis. Comun. Image Represent.*, 25(1):195–206, Jan. 2014.

[7] H. Iwama, D. Muramatsu, Y. Makihara, and Y. Yagi. Gait verification system for criminal investigation. *IPSJ Trans. on Computer Vision and Applications*, 5:163–175, Oct. 2013.

[8] H. Iwama, M. Okumura, Y. Makihara, and Y. Yagi. The ou-isir gait database comprising the large population dataset and performance evaluation of gait recognition. *IEEE Transactions on Information Forensics and Security*, 7(5):1511–1521, Oct. 2012.

[9] W. Kusakunniran, Q. Wu, J. Zhang, and H. Li. Cross-view and multi-view gait recognitions based on view transformation model using multi-layer perceptron. *Pattern Recognition Letters*, 33(7):882–889, 2012.

[10] W. Kusakunniran, Q. Wu, J. Zhang, and H. Li. Gait recognition under various viewing angles based on correlated motion regression. *IEEE Transactions on Circuits and Systems for Video Technology*, 22(6):966–980, 2012.

[11] N. Liu, J. Lu, and Y.-P. Tan. Joint subspace learning for view-invariant gait recognition. *IEEE Signal Processing Letters*, 18(7):431–434, 2011.

[12] Z. Liu and S. Sarkar. Simplest representation yet for gait recognition: Averaged silhouette. In *Proc. of the 17th International Conference on Pattern Recognition*, volume 1, pages 211–214, Aug. 2004.

[13] J. Lu and Y.-P. Tan. Uncorrelated discriminant simplex analysis for view-invariant gait signal computing. *Pattern Recognition Letters*, 31(5):382–393, 2010.

[14] N. Lynnerup and P. Larsen. Gait as evidence. *IET Biometrics*, 3(2):47–54, 6 2014.

[15] Y. Makihara, H. Mannami, A. Tsuji, M. Hossain, K. Sugiura, A. Mori, and Y. Yagi. The ou-isir gait database comprising the treadmill dataset. *IPSJ Transactions on Computer Vision and Applications*, 4:53–62, Apr. 2012.

[16] Y. Makihara, M. Okumura, H. Iwama, and Y. Yagi. Gait-based age estimation using a whole-generation gait database. In *Proc. of the Int. Joint Conf. on Biometrics (IJCB2011)*, pages 1–6, Washington D.C., USA, Oct. 2011.

[17] Y. Makihara, M. Okumura, Y. Yagi, and S. Morishima. The online gait measurement for characteristic gait animation synthesis. In R. Shumaker, editor, *Proc. of Human Computer Interaction Int. 2011, Virtual and Mixed Reality - New Trends*, volume 6773 of *Lecture Notes in Computer Science*, pages 325–334, Orlando, FL, USA, 2011. Springer.

[18] Y. Makihara, R. Sagawa, Y. Mukaigawa, T. Echigo, and Y. Yagi. Gait recognition using a view transformation model in the frequency domain. In *Proc. of the 9th European Conference on Computer Vision*, pages 151–163, Graz, Austria, May 2006.

[19] Y. Makihara, A. Tsuji, and Y. Yagi. Silhouette transformation based on walking speed for gait identification. In *Proc. of the 23rd IEEE Conf. on Computer Vision and Pattern Recognition*, San Francisco, CA, USA, Jun 2010.

[20] Y. Makihara and Y. Yagi. Silhouette extraction based on iterative spatio-temporal local color transformation and graph-cut segmentation. In *Proc. of the 19th Int. Conf. on Pattern Recognition*, pages 1–4, Tampa, Florida USA, Dec. 2008.

[21] A. Mansfield and J. Wayman. Best practices in testing and reporting performance of biometric devices, version 2.01. *National Physical Laboratory Report CMSC*, 14(2):1–36, Aug. 2002.

[22] A. Mansur, Y. Makihara, R. Aqmar, and Y. Yagi. Gait recognition under speed transition. In *Computer Vision and Pattern Recognition (CVPR), 2014 IEEE Conference on*, pages 2521–2528, June 2014.

[23] A. Mansur, Y. Makihara, D. Muramatsu, and Y. Yagi. Cross-view gait recognition using view-dependent discriminative analysis. In *The 2nd IEEE Int. Joint Conf. on Biometrics (IJCB 2014)*, pages 1–8, Sept 2014.

[24] R. Martin-Felez and T. Xiang. Uncooperative gait recognition by learning to rank. *Pattern Recognition*, 47(12):3793 – 3806, 2014.

[25] D. Muramatsu, A. Shiraishi, Y. Makihara, M. Uddin, and Y. Yagi. Gait-based person recognition using arbitrary view transformation model. *IEEE Trans. on Image Processing*, 24(1):140–154, Jan 2015.

[26] M. S. Nixon, T. N. Tan, and R. Chellappa. *Human Identification Based on Gait*. Int. Series on Biometrics. Springer-Verlag, Dec. 2005.

[27] S. Sarkar, J. Phillips, Z. Liu, I. Vega, P. G. ther, and K. Bowyer. The humanid gait challenge problem: Data sets, performance, and analysis. *IEEE Trans. of Pattern Analysis and Machine Intelligence*, 27(2):162–177, 2005.

[28] J. Shutler, M. Grant, M. Nixon, and J. Carter. On a large sequence-based human gait database. In *Proc. of the 4th Int. Conf. on Recent Advances in Soft Computing*, pages 66–71, Nottingham, UK, Dec. 2002.

[29] T. Wada, Y. Matsumura, S. Maeda, and H. Shibuya. Gaussian process regression with dynamic active setand its application to anomaly detection. In *The 9th International Conference on Data Mining*, Jul. 2013.

[30] S. Yu, D. Tan, and T. Tan. A framework for evaluating the effect of view angle, clothing and carrying condition on gait recognition. In *Proc. of the 18th Int. Conf. on Pattern Recognition*, volume 4, pages 441–444, Hong Kong, China, Aug. 2006.